# Lectin-Recognizable MOF Glyconanoparticles: Supramolecular Glycosylation of ZIF-8 Nanocrystals by Sugar-Based Surfactants

Rodrigo E. Giménez, Esteban Piccinini, Omar Azzaroni,*[ID] and Matías Rafti*[ID]

Dto. de Química, Fac. de Cs. Exactas, Instituto de Investigaciones Fisicoquímicas Teóricas y Aplicadas (INIFTA), Universidad Nacional de La Plata, CONICET, Calle 64 y Diag. 113, 1900 La Plata, Argentina

ABSTRACT: A strategy toward the integration of highly functional microporous materials, such as metal-organic frameworks (MOFs), in composites via biochemical recognition interactions is presented. Postsynthetic modification of zeolitic-imidazolate framework-8 MOF nanocrystals with a maltose-exposing biocompatible surfactant (the so-called "Glyco-MOFs") was performed to confer affinity toward lectin protein concanavalin A. The addition of small amounts of concanavalin A to the colloidal Glyco-MOF dispersion triggers the aggregation of these units into self-limited size supramolecular architectures directed by specific sugar−lectin binding interactions.
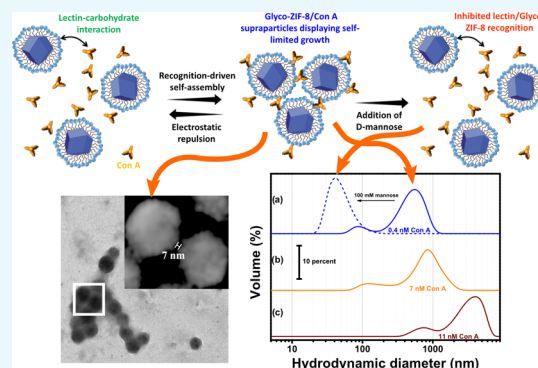
INTRODUCTION

Recently, a new class of organic−inorganic crystalline porous materials, known as metal-organic frameworks (MOFs), has emerged. MOFs are highly ordered structures that can be described in terms of metal ions as centers (or metal-containing clusters), connected coordinately by multidentate organic chelating agents acting as linkers.[1−4] Due to the overwhelming number of organic linkers and metal combinations possible, a broad variety of materials with many different features can be obtained. Among many interesting characteristics, MOFs exhibit high surface areas, a wide range of pore sizes and shapes, and a great variety of chemical functionalities exposed in the pore.[5] Zeolitic-imidazolate frameworks (or ZIFs) constitute a particularly well-characterized and studied MOF subclass. ZIFs can be described as M−Im−M tridimensional porous networks, where M stands for tetrahedrally coordinated Zn^{2+} or Co^{2+} metal ions and Im represents an imidazolate or imidazolate-derived N-bidentate organic linker.[6,7] Due to its straightforward synthesis methods, high surface areas, and relatively high stability (both thermal and toward hydrolysis in neutral aqueous solutions), ZIF-8 (constituted by Zn^{2+} ions and 2-methylimidazole (HmIm) bidentate linker) is an appealing material widely used for water-based applications, including many examples related to biomedicine and nanobiotechnology.[8−17]

Much effort has been devoted in MOF research to the development of strategies allowing modification of their bulk structure and pore surface chemistry, to, e.g., confer differential affinity toward energy or environmentally relevant adsorbates,[18] or introducing structural defects, which could act as catalytic sites or create some degree of mesoporosity in an otherwise strictly microporous framework.[19] Modification of external surface in MOF films and nanocrystals has received relatively less attention,[20−26] although it provides an ideal tool for many

interesting applications, as increasingly recognized by the nanobioscience research community.[27] To mention one of the many examples, it has been recently reported that an immune system recognition response decrease was caused by surface-confined positioning of a biopolymer on MOF nanocrystals.[28,29]

Carbohydrates and carbohydrate-containing polymers constitute a predominant class of biologically relevant molecules acting in a multitude of biochemical processes, such as cellular recognition, inflammation, and signal transmission. The ability of carbohydrate-exposing synthetic materials to mimic such functional response has attracted increasing interest of the biomaterials community.[30,31] Carbohydrates can form many hydrogen bonds, an interesting feature for further developments as a tool in supramolecular chemistry, due to the possibility of interaction with other carbohydrates and proteins.[32] The presence of multiple surface-exposed carbohydrates increases the binding strength conferred by individual interactions to yield synergetic multivalent interactions.[33,34] Supramolecular assemblies exposing carbohydrates in their surface include among other organic macrocycles (such as cyclodextrins (CDs)), glycoclusters and glycodendrimers, and glycopolymers.[35] Particularly, in recent years, we have witnessed an increased interest in the combination of nanomaterials and carbohydrates. Research efforts on this matter are often referred to as glyconanotechnology, a term popularized by Penadés and co-workers.[31] Great strides in glyconanotechnology have been made as a result of the creation of different bioactive glyconanostructures for various health-related applications, such as drug delivery, gene therapy, pathogen detection, toxin

inhibition, and lectin-based biosensors.[36−40] In this sense, advances oriented to the incorporation of such functionalities in MOFs and MOF-containing composites have been focused on replacing usual organic linkers with carbohydrate supramolecular assemblies, such as cyclodextrins (CDs), yielding edible porous materials, the so-called CD-MOFs.[41−44]

Alkyl-polyglucosydes (APG) are nontoxic, sugar-based surfactants[45] with low surface tension and good electrolyte tolerance. An example of APG is the *n*-dodecyl *β*-D-maltoside (DDM). DDM adsorbs strongly over hydrophobic surfaces forming monolayers.[46] DDM monolayers allow its use as a stabilizing agent for colloidal suspensions of nonpolar nanoparticles in polar solvents, adding the interesting feature of surface positioning of hydrophilic maltoside residues.

In this work, we have used a simple and straightforward noncovalent surface modification of ZIF-8 MOF nanocrystals to create surface-exposed sugar moieties, which are meant to confer the lectin-recognition properties. Our studies were aimed to explore the possibility of forming colloidal sugar-modified ZIF-8 nanocrystals, which can offer the possibility of recognition-driven assembly in the presence of concanavalin A (Con A), a well-studied lectin protein commonly used for in vitro biological essays.[35,37] We demonstrate that DDM serves as a suitable dispersing and stabilizing agent for ZIF-8 colloids; furthermore, its presence significantly affects the interactions between ZIF-8 nanocrystals and Con A. Due to the presence of sugar moieties exposed at ZIF-8 surface, the addition of small amounts of Con A to the colloidal dispersion triggers the aggregation of functionalized ZIF-8 nanocrystals as a result of specific sugar−lectin binding interactions.

■ RESULTS AND DISCUSSION

Dynamic Light Scattering (DLS). Glyco-ZIF-8 colloidal suspensions formation was in situ monitored via DLS. Figure 1
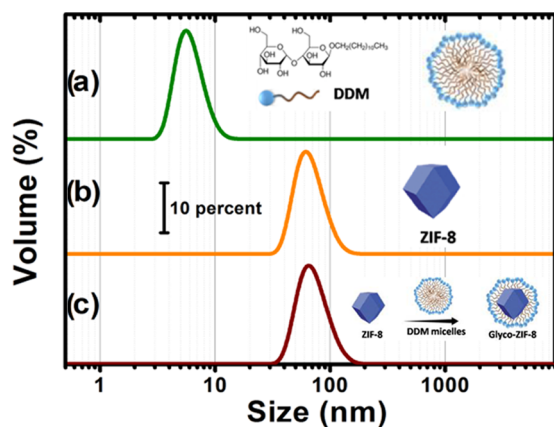

Figure 1. Hydrodynamic diameter distribution measured by DLS for: (a) 2 mM DDM solution, which yields monodisperse micelles; (b) ZIF-8 nanocrystals formed after direct mixing of precursors; and (c) ZIF-8 nanocrystals colloidal suspension obtained in (b) with 2 mM DDM solution. For each plot, a schematic illustration of the system obtained is also presented.

shows the final size distributions obtained for the following systems: (a) 2 mM DDM, (b) ZIF-8 formed by direct mixing as discussed below, and (c) a mixture of ZIF-8 colloidal suspension obtained in (a) with DDM for the same final concentration.

Shortly after mixing ZIF-8 colloidal nanocrystals suspension and DDM solution for a final 2 mM concentration, a remarkably

size-monodisperse population emerges, with mean hydrodynamic diameter slightly larger than that measured for ZIF-8 alone. Furthermore, DDM micelles of approximately 9 nm presented in Figure 1a disappear, which suggests that DDM micelles spontaneously disassemble and adsorb onto ZIF-8 nanocrystals, yielding Glyco-ZIF-8 colloidal suspensions.

To explore the effect of lectin−sugar affinity on the possibility of creating supramolecular aggregates, we added Con A to the colloidal suspension of Glyco-ZIF-8. DLS results of such experiment can be observed in Figure 2.
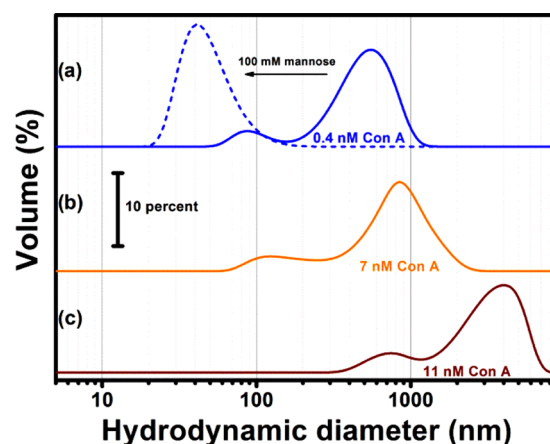

Figure 2. Hydrodynamic diameter distribution measured by DLS of Glyco-ZIF-8/Con A supraparticles for different lectin final concentrations: (a) 0.4 nM Con A (solid line −), 0.4 nM Con A added after addition of 100 nM D-mannose (dashed line --), (b) 7 nM Con A, and (c) 11 nM Con A.

It can be clearly observed from Figure 2a (solid line) that the addition of Con A (even at nanomolar concentrations) leads to the formation of self-assembled Glyco-ZIF-8/Con A supraparticles showing a self-limited growth. Understanding why and how the self-assembly process occurs in a self-limited fashion requires a detailed assessment of the driving forces operating between building blocks.[47] In this regard, Kotov et al. demonstrated that this interesting behavior can be described in terms of a delicate interplay between repulsive and attractive forces, i.e., thermodynamically controlled growth reaches a limit when repulsive interactions between formed supraparticles and nanoprecursors exceeds the attractive forces leading to formation in the first place. Different from the commonly used kinetically controlled template-assisted supraparticle growth, the above-described strategy allows for fine tuning via environmental variables (e.g., pH, temperature, ionic strength).[48,49] This control strategy was tested for the formation of all-inorganic supraparticles and hybrid supraparticles, where the driving forces for the assembly were repulsive electrostatic interactions and attractive van der Waals interactions. Recently, the approach has been extended for the synthesis of glycoenzyme−lectin self-limited supraparticles that presented lectin−carbohydrate recognition and electrostatic interaction as the main attractive and repulsive forces, respectively.[50] To evaluate the importance of lectin−carbohydrate recognition interactions in the Glyco-ZIF-8/Con A supraparticles assembly, we studied the process in the presence of 100 mM D-mannose, acting as competing agent for the Con A binding sites (Figure 2a, dashed line). When mannose is added before Con A, lectin/Glyco-ZIF-8 assembly results were inhibited, which strongly

suggest the crucial role of carbohydrate recognition for supraparticle formation. An important parameter for the assessment of further applications of these supraparticles is the association constant (K_a), which can be expected to lie in the range of $1 \times 10^7 - 1 \times 10^9$ M^{-1} based on already reported values for the affinity between maltose-grafted nanoparticles and Con A protein.[51,52] Due to the effect of multivalent recognition, the observed affinity between maltose-grafted nanoparticles and Con A can be several orders of magnitude higher than the values observed for interaction between free maltose and Con A (K_a = 2.1×10^3 M^{-1}).[53]

ζ-Potential measurements were carried out to explore the effect of surface modifications on ZIF-8 nanocrystals. Figure 3

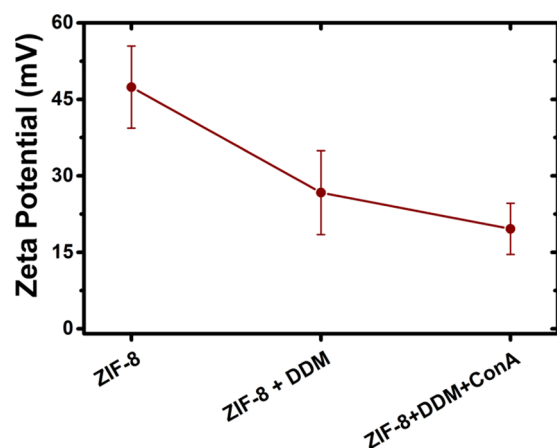**Figure 3.** ζ potential measurements of ZIF-8, Glyco-ZIF-8 prepared with DDM, and Glyco-ZIF-8/Con A supraparticles with a final Con A concentration of 0.4 nM.

shows the observed evolution of surface charge. According to what can be expected from surface functionalization, after DDM coating, surface charge diminishes due to partial shielding; further decrease can be observed as Con A is added to the Glyco-ZIF-8 colloidal suspension forming supraparticles.

It should be noted that Glyco-ZIF-8 supraparticles remain positively charged, whereas lectin protein is negatively charged for the conditions used in the experiments. Because of the presence of oppositely charged constituents, it would be expected that only attractive (van der Waals, electrostatic, and biorecognition) forces participate, rendering it very difficult to achieve a self-limited growth. Nevertheless, we found that the

extent of agglomeration, i.e., the hydrodynamic diameter and the ζ potential of the supraparticles, strongly depends on the [Con A]/[Glyco-ZIF-8] ratio (Figures 2 and 3). In particular, we observed that self-limited and stable colloidal systems were obtained when the [Con A]/[Glyco-ZIF-8] ratio leads to positively charged supraparticles. For example, the addition of 0.4 nM Con A resulted in supraparticles with a ζ-potential value of +20 mV. By increasing Con A concentration, ζ-potential of the supraparticles decreased while average size increased (see Figure 2a−c).

Above 11 nM Con A concentration, the resultant ζ potential of the supraparticle approaches zero and full agglomeration can be expected as actually occurred. Similar behavior was observed by other authors for the self-assembly of positively charged proteins and negatively charged Au nanoparticles, which was discussed in detail by Moerz et al. in terms of electrostatic repulsion and van der Waals attractive interactions.[54] Scheme 1 shows a representation of recognition-driven self-assembly as discussed above.

Transmission Electron Microscopy (TEM). TEM images confirming the morphology and size distribution of the colloidal suspensions measured after DDM functionalization were obtained. Figure 4 displays an example of such size distributions, and particle size analysis shows a monodisperse population centered at 83 ± 13 nm diameter.

Furthermore, calculated size distributions of Glyco-ZIF-8 after Con A addition in Figure 4 are bimodal; this result is in line with the presence of both populations of nanoprecursors and supraparticles, as observed in DLS (see Figure 2). Another interesting observation that can be extracted from typical TEM images, such as those presented in Figure 4, is an estimation of the interparticle distance between Con A-assembled Glyco-ZIF-8 unit, which is in the range of ≈10 nm. Although the ex situ character of TEM measurements does not allow for a direct comparison with actual values inferred from DDM and Con A molecular dimensions, both the determined size of supraparticle assemblies and the interparticle distance in Glyco-ZIF-8 are in line with in situ DLS measurements and agree reasonably well with the expected values for DDM-Con A spacers, ≈7 nm (see Scheme 1).[50,55] To further characterize the chemical composition of DDM-functionalized ZIF-8 nanocrystals observed by TEM, we performed energy-dispersive X-ray spectroscopy (EDS) and measured elemental composition (Zn, N, and O) profile along a transversal direction, as shown in Figure 5. The presence of Zn and N inside the nanocrystals correlates well with

Scheme 1. Representation of the Recognition-Driven Self-Assembly of Glyco-ZIF-8 and Con A Leading to the Formation of Supraparticles with Self-Limited Growth, and Disassembly Tiggered by Competitive Agent
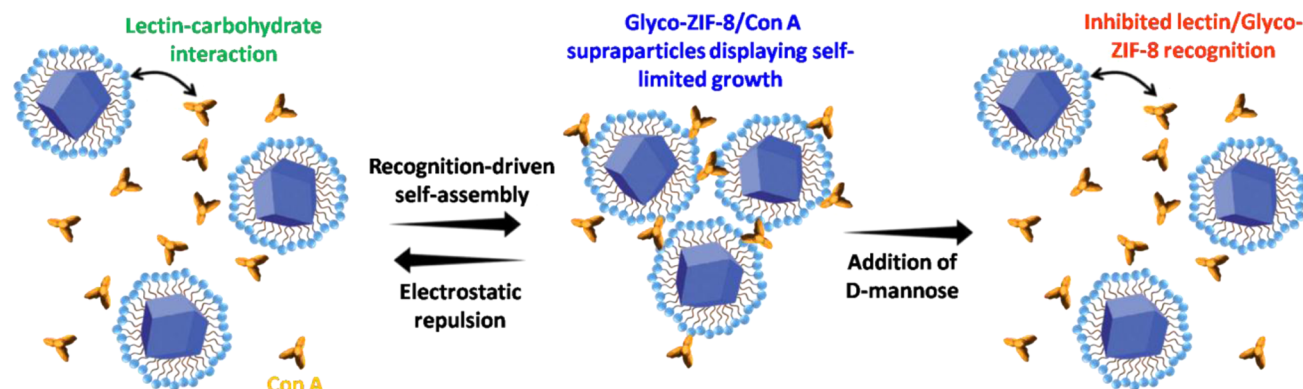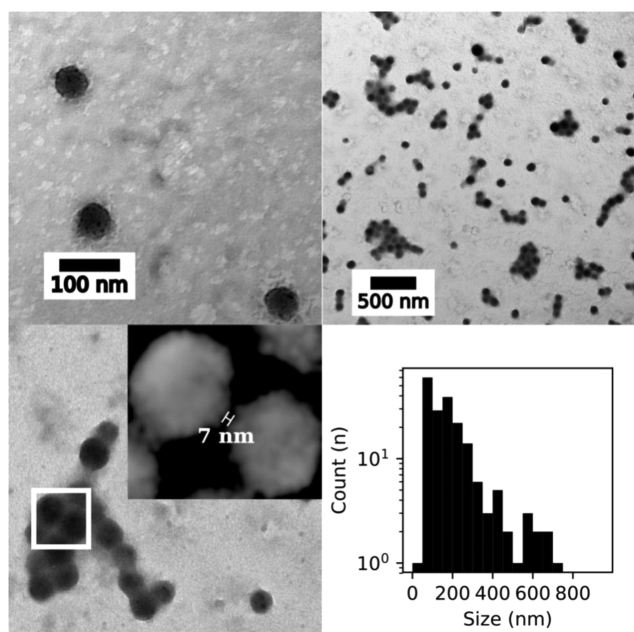
Figure 4. (Top) TEM images of Glyco-MOFs before (left) and after (right) 7 nM Con A addition. (Bottom) Distance between two Glyco-ZIF-8 nanocrystals in the presence of Con A (left), and size distribution (right) for the same experiment (7 nM Con A) calculated using the longest distance between any two points on the supraparticle.

the known chemical composition of metallic center (Zn) and the linker (2-methylimidazolate) constituting ZIF-8 structure. It is interesting to note that (although rather weak due to the number of DDM molecules present on the nanocrystal surface), in line with DLS and quartz crystal microbalance (QCM) experiments, there is a signal attributable to oxygen, which provides further indication of DDM surface positioning.

Crystalline Structure via X-ray Diffraction (XRD) and Thermogravimetric Analysis (TGA) Experiments. X-ray diffractograms were carried out to characterize the crystalline structure of synthesized materials and to assess its stability toward aqueous environments used in the supraparticle assembly; Figure 6 summarizes the results obtained. A comparison with calculated ZIF-8 diffractogram from reported structure is also presented, which further confirms the presence of the material after the assembly procedure.
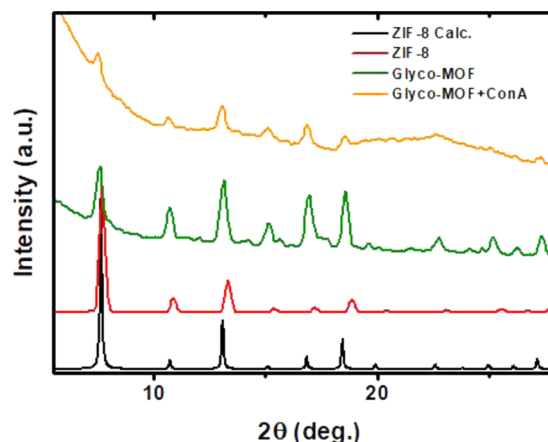

Figure 6. X-ray diffractograms obtained for the as-prepared material, DDM-functionalized (Glyco-MOF), and Con A-assembled supraparticles (Glyco-MOF + Con A). In all cases, structures can be safely assumed to retain ZIF-8 characteristic reflections and thus crystal structure.

Figure 7 allows for a comparison between the weight loss profiles observed in TGA experiments for ZIF-8 alone and
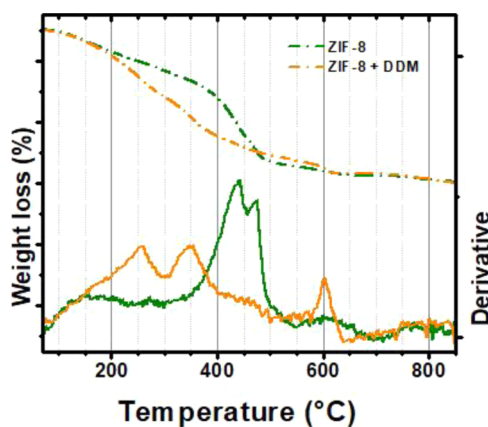

Figure 7. Weight loss profile and its corresponding derivative for ZIF-8 nanocrystals and DDM-functionalized ZIF-8. Earlier weight loss between 200 and 300 °C points toward the presence of DDM, which is not present in ZIF-8 thermograms.
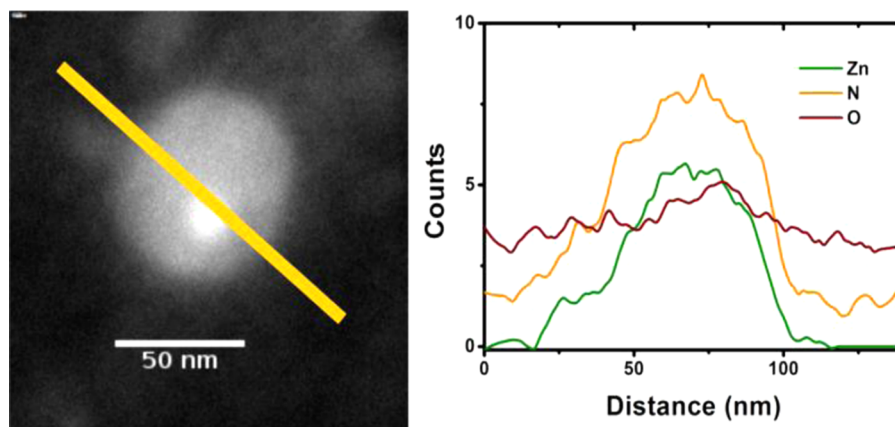

Figure 5. (Left) TEM images of ZIF-8 + DDM nanocrystal and (right) elemental line profile along the path shown in TEM image obtained from EDS.

DDM-functionalized ZIF-8 nanocrystals. It is expected that when a labile component is present in the structure, an earlier weight loss would appear (DDM surfactant decomposition); this was observed in Figure 7 with DDM decomposition between 200 and 300 °C.

Quartz Crystal Microbalance (QCM) Experiments. To bring further support to the proposed lectin–carbohydrate-driven assembly of Glyco-ZIF-8 units, the quartz crystal microbalance (QCM) technique was used. Initially, mannosylated crystals prepared using the protocols described in the Experimental Section below were incubated with Con A solution to position a lectin monolayer on the sensor surface. After rinsing with Milli-Q water and drying with N_2, the Con A adsorption resulted in a frequency decrease of −18 Hz. Frequency change (Δf) measured using QCM can be converted to surface mass coverage (Γ) using the Sauerbrey equation, and the measured value translates to 318 ng/cm^2, which is in good agreement with the previously reported values for Con A layer (Γ_{ConA}) formation.[56,57] Subsequently, the Con A-modified crystal was incubated in Glyco-ZIF-8 colloidal suspension. Figure 8 shows Δf time evolution during the assembly of the
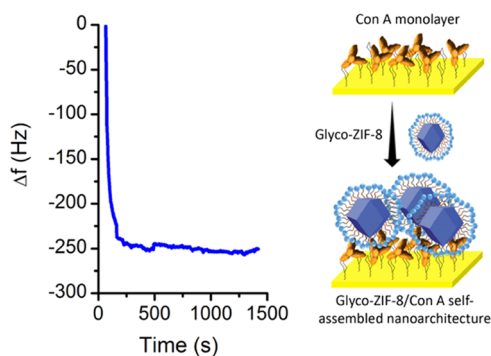

Figure 8. Quartz crystal microbalance in situ monitoring of the glycosylated MOF assembly onto a Con A-modified crystal (left). Frequency change (Δf) time evolution.

DDM-functionalized ZIF-8 nanocrystals mediated by lectin–carbohydrate recognition. A rapid assembly process can be seen since most of the Glyco-ZIF-8 adsorption occurs in less than 2 min (compared to the time range observed for similar mediated assemblies of ZIF-8 nanocrystals, which take more than 2 h to reach final stages).[20]

The Glyco-ZIF-8/Con A architecture showed good stability during immersion in deionized water. The frequency change between the Glyco-ZIF-8/Con A-modified crystal and the Con A-modified crystal (both measured in dry conditions) was −60 Hz, i.e., a Γ_{MOF} of 1060 ng/cm^2.

CONCLUSIONS

Conditions for stability and surface functionalization of ZIF-8 MOF nanocrystals using a biocompatible surfactant (DDM) were determined. As a proof of concept, Glyco-ZIF-8 units thus synthesized (i.e., maltose-exposing ZIF-8 nanocrystals) were assembled using affinity of lectin protein Con A toward maltose. The supraparticles obtained display a self-limited size as a result of lectin–carbohydrate recognition, and accordingly, the interactions governing the process were found to be not only effective but also specific (QCM control experiments carried out using ZIF-8 nanocrystals without DDM surface modification were observed to produce frequency changes nearly an order of

magnitude lower than that obtained using DDM-modified ZIF-8).

Having in mind that ZIF-8 was proven in the past to possess a number of interesting features (e.g., its ability to selectively adsorb O_2 from aqueous environments, or the possibility of placing different guest molecules on the available porosity), the hereby presented possibility of synthesizing Glyco-ZIF-8/Con A self-limited supraparticles opens the path for a number of interesting applications in the field of functional nano-biomaterials. With little modifications, the approach presented can be applied to different recognition-driven systems, using diverse MOFs and biomolecules.

■ EXPERIMENTAL SECTION

Materials Used, Synthesis, and Procedures. All reagents were used as supplied by manufacturer (Sigma-Aldrich), namely, zinc nitrate hexahydrate, 2-methylimidazole (HmIm), n-dodecyl β-D-maltoside (DDM), concanavalin A (Con A) from *Canavalia ensiformis* (Jack bean), α-D-mannopyranosyl-phenyl-isothiocyanate, cysteamine hydrochloride, N-(2-hydroxyethyl)-piperazine-N′-ethanesulfonic acid (HEPES), and D-mannose (Sigma-Aldrich). Gold-coated quartz crystal QCM substrates were provided by Stanford Research Systems. DLS and QCM experiments were carried out at 20 °C. A 1 μM Con A stock solution was prepared in the presence of 100 mM KCl, 20 mM HEPES (pH 7.4), 0.5 mM $CaCl_2$, and 0.5 mM $MnCl_2$.

Glyco-ZIF-8 Synthesis. ZIF-8 nanocrystals were prepared by mixing aqueous solutions of the precursors. Briefly, 4.5 mL volume of 50 mM HmIm solution was quickly added to 0.5 mL of 25 mM metal precursor solution to obtain ZIF-8 nanocrystals colloid after 45−60 min total reaction time. Afterward, 10 mM stock solution of DDM was used to modify the ZIF-8 colloidal suspension (DDM final concentration in the mixture, 2 mM) to yield Glyco-MOF nanocrystals.

Synthesis of Con A/Glyco-MOF Supraparticles. Supraparticles made of Concanavalin A (Con A) and Glyco-MOF were assembled in aqueous media by dropwise addition of Con A solution to a colloidal suspension of Glyco-MOF obtained as stated above and under smooth stirring.

QCM and E-QCM Experiments. QCM measurements were performed with a QCM200 Quartz Cristal Microbalance equipped with Gold QCM25 5 MHz oscillators (sensitivity factor: 56.6 Hz cm^2/μg) (Stanford Research Systems). Determinations were performed with quiescent solutions in a Teflon cell. The crystals were cleaned by immersion into a 1:1:5 volume ratio solution of hydrogen peroxide (30%), ammonia (25%), and deionized water kept at 75 °C for 5 min. Then, gold surface was modified with mannose motif as previously reported.[50] To study the assembly kinetics, the frequency was in situ monitored during adsorption of each component (Con A and ZIF-8 nanocrystals). Moreover, the mass surface coverage (Γ) was estimated by comparing the frequency before and after the assembly in dry conditions and assuming that the system can be understood in terms of Sauerbrey's model.[58]

Dynamic Light Scattering (DLS) Experiments for Size and ζ-Potential Determination. Hydrodynamic diameters and polydispersity were determined by dynamic light scattering (DLS) experiments using a Malvern Zetasizer ZS apparatus. We used a 633 nm He−Ne laser and backscattered detection optic arrangement, i.e., detector placed at 7° with respect to the incident light beam. All of the measurements were carried out in 7 mM HEPES pH 7.4 buffer containing 35 mM KCl. ζ potential measurements were determined from three independent

experiments to ensure reproducibility, using capillary cells (Malvern Instruments) with a drive cell voltage of 30 V. For the ζ potential calculations, the Smoluchowski approximation of the Henry equation was employed.

TEM and EDS. Transmission electron microscopy (TEM) images were obtained with a JEM 1200 EX II (JEOL Ltd.) equipped with a digital camera Erlangshen ES1000 W, model 785 (Gatan Inc.). The samples were observed under an accelerating voltage of 100 kV. Energy-dispersive spectrum (EDS) mapping was carried out using a Talos TEM (FEI; Talos F200X 80−200). Size distributions and image analysis were carried out using BioImageXD software.[59]

Thermogravimetric Analysis (TGA). Thermogravimetric analysis was carried out using TGA Q500 (TA Instruments), with a N_2 flow of 20 mL/min, at 5 °C/min heating rate with Pt pans.

X-ray Diffraction (XRD). Calculated X-ray diffraction patterns were obtained from Cambridge Crystallographic Data Base ZIF-8 files using Mercury software.[60] Diffraction experiments on the synthesized materials were recorded at room temperature under ambient conditions on a Phillips X'Pert-1 diffractometer.

■ AUTHOR INFORMATION

Corresponding Authors
*E-mail: azzaroni@inifta.unlp.edu.ar (O.A.).
*E-mail: mrafti@quimica.unlp.edu.ar (M.R.).

ORCID Ⓘ
Omar Azzaroni: 0000-0002-5098-0612
Matías Rafti: 0000-0003-3393-358X

Notes
The authors declare no competing financial interest.

■ ACKNOWLEDGMENTS

■ REFERENCES

(1) Yaghi, O. M.; Li, G.; Li, H. Selective Binding and Removal of Guests in a Microporous Metal−organic Framework. *Nature* **1995**, *378*, 703−706.

(2) Hoskins, B.; Robson, R. Infinite Polymeric Frameworks Consisting of Three Dimensionally Linked Rod-like Segments. *J. Am. Chem. Soc.* **1989**, *111*, 5962−5964.

(3) Furukawa, H.; Cordova, K. E.; O'Keeffe, M.; Yaghi, O. M. The Chemistry and Applications of Metal-Organic Frameworks. *Science* **2013**, *341*, No. 1230444.

(4) Férey, G. Hybrid Porous Solids: Past, Present, Future. *Chem. Soc. Rev.* **2008**, *37*, 191−214.

(5) Stock, N.; Biswas, S. Synthesis of Metal-Organic Frameworks (MOFs): Routes to Various MOF Topologies, Morphologies, and Composites. *Chem. Rev.* **2012**, *112*, 933−969.

(6) Wang, B.; Côté, A. P.; Furukawa, H.; O'Keeffe, M.; Yaghi, O. M. Colossal Cages in Zeolitic Imidazolate Frameworks as Selective Carbon Dioxide Reservoirs. *Nature* **2008**, *453*, 207−211.

(7) Park, K. S.; Ni, Z.; Côté, A. P.; Choi, J. Y.; Huang, R.; Uribe-Romo, F. J.; Chae, H. K.; O'Keeffe, M.; Yaghi, O. M. Exceptional Chemical and Thermal Stability of Zeolitic Imidazolate Frameworks. *Proc. Natl. Acad. Sci. U.S.A.* **2006**, *103*, 10186−10191.

(8) Horcajada, P.; Chevreau, H.; Heurtaux, D.; Benyettou, F.; Salles, F.; Devic, T.; Garcia-Marquez, A.; Yu, C.; Lavrard, H.; Dutson, C. L.; et al. Extended and Functionalized Porous iron(III) Tri- or Dicarboxylates with MIL-100/101 Topologies. *Chem. Commun.* **2014**, *50*, 6872−6874.

(9) McKinlay, A. C.; Morris, R. E.; Horcajada, P.; Férey, G.; Gref, R.; Couvreur, P.; Serre, C. BioMOFs: Metal-Organic Frameworks for Biological and Medical Applications. *Angew. Chem., Int. Ed.* **2010**, *49*, 6260−6266.

(10) Huxford, R. C.; Rocca, J. D.; Lin, W. Metal−Organic Frameworks as Potential Drug Carriers. *Curr. Opin. Chem. Biol.* **2010**, *14*, 262−268.

(11) Cunha, D.; Yahia, M. B.; Hall, S.; Miller, S. R.; Chevreau, H.; Elkaïm, E.; Maurin, G.; Horcajada, P.; Serre, C. Rationale of Drug Encapsulation and Release from Biocompatible Porous Metal−Organic Frameworks. *Chem. Mater.* **2013**, *25*, 2767−2776.

(12) Liu, D.; Huxford, R. C.; Lin, W. Phosphorescent Nanoscale Coordination Polymers as Contrast Agents for Optical Imaging. *Angew. Chem., Int. Ed.* **2011**, *50*, 3696−3700.

(13) Rowe, M. D.; Tham, D. H.; Kraft, S. L.; Boyes, S. G. Polymer-Modified Gadolinium Metal-Organic Framework Nanoparticles Used as Multifunctional Nanomedicines for the Targeted Imaging and Treatment of Cancer. *Biomacromolecules* **2009**, *10*, 983−993.

(14) Zhu, X.; Gu, J.; Wang, Y.; Li, B.; Li, Y.; Zhao, W.; Shi, J. Inherent Anchorages in UiO-66 Nanoparticles for Efficient Capture of Alendronate and Its Mediated Release. *Chem. Commun.* **2014**, *50*, 8779−8782.

(15) Wang, W.; Wang, L.; Li, Z.; Xie, Z. BODIPY-Containing Nanoscale Metal-Organic Frameworks for Photodynamic Therapy. *Chem. Commun.* **2016**, *52*, 5402.

(16) Zhao, H.-X.; Zou, Q.; Sun, S.-K.; Yu, C.; Zhang, X.; Li, R.-J.; Fu, Y. Theranostic Metal-Organic Framework Core-Shell Composites for Magnetic Resonance Imaging and Drug Delivery. *Chem. Sci.* **2016**, *7*, 5294.

(17) Horcajada, P.; Gref, R.; Baati, T.; Allan, P. K.; Maurin, G.; Couvreur, P.; Férey, G.; Morris, R. E.; Serre, C. Metal−Organic Frameworks in Biomedicine. *Chem. Rev.* **2012**, *112*, 1232−1268.

(18) Flaig, R. W.; Popp, T. M. O.; Fracaroli, A. M.; Kapustin, E. A.; Kalmutzki, M. J.; Altamimi, R. M.; Fathieh, F.; Reimer, J. A.; Yaghi, O. M. The Chemistry of CO_2 Capture in an Amine-Functionalized Metal−Organic Framework under Dry and Humid Conditions. *J. Am. Chem. Soc.* **2017**, *139*, 12125−12128.

(19) Fang, Z.; Bueken, B.; De Vos, D. E.; Fischer, R. A. Defect-Engineered Metal-Organic Frameworks. *Angew. Chem., Int. Ed.* **2015**, *54*, 7234−7254.

(20) Segovia, G. M.; Tuninetti, J. S.; Moya, S.; Picco, A. S.; Ceolín, M. R.; Azzaroni, O.; Rafti, M. Cysteamine-Modified ZIF-8 Colloidal Building Blocks: Direct Assembly of Nanoparticulate MOF Films on Gold Surfaces via Thiol Chemistry. *Mater. Today Chem.* **2018**, *8*, 29−35.

(21) Sindoro, M.; Yanai, N.; Jee, A.-Y.; Granick, S. Colloidal-Sized Metal−Organic Frameworks: Synthesis and Applications. *Acc. Chem. Res.* **2014**, *47*, 459−469.

(22) Wang, S.; Morris, W.; Liu, Y.; McGuirk, C. M.; Zhou, Y.; Hupp, J. T.; Farha, O. K.; Mirkin, C. A. Surface-Specific Functionalization of Nanoscale Metal-Organic Frameworks. *Angew. Chem., Int. Ed.* **2015**, *54*, 14738−14742.

(23) McGuire, C. V.; Forgan, R. S. The Surface Chemistry of Metal−organic Frameworks. *Chem. Commun.* **2015**, *51*, 5199−5217.

(24) Wang, Z.; Cohen, S. M. Postsynthetic Modification of Metal−organic Frameworks. *Chem. Soc. Rev.* **2009**, *38*, 1315.

(25) Kim, M.; Cahill, J. F.; Fei, H.; Prather, K. A.; Cohen, S. M. Postsynthetic Ligand and Cation Exchange in Robust Metal−Organic Frameworks. *J. Am. Chem. Soc.* **2012**, *134*, 18082−18088.

(26) Kondo, M.; Furukawa, S.; Hirai, K.; Kitagawa, S. Coordinatively Immobilized Monolayers on Porous Coordination Polymer Crystals. *Angew. Chem., Int. Ed.* **2010**, *49*, 5327−5330.

(27) Horcajada, P.; Chalati, T.; Serre, C.; Gillet, B.; Sebrie, C.; Baati, T.; Eubank, J. F.; Heurtaux, D.; Clayette, P.; Kreuz, C.; et al. Porous

Metal-Organic-Framework Nanoscale Carriers as a Potential Platform for Drug Delivery and Imaging. *Nat. Mater.* **2010**, *9*, 172−178.

(28) Wuttke, S.; Braig, S.; Preiß, T.; Zimpel, A.; Sicklinger, J.; Bellomo, C.; Rädler, J. O.; Vollmar, A. M.; Bein, T. MOF Nanoparticles Coated by Lipid Bilayers and Their Uptake by Cancer Cells. *Chem. Commun.* **2015**, *51*, 15752−15755.

(29) Zimpel, A.; Preiß, T.; Röder, R.; Engelke, H.; Ingrisch, M.; Peller, M.; Rädler, J. O.; Wagner, E.; Bein, T.; Lächelt, U.; et al. Imparting Functionality to MOF Nanoparticles by External Surface Selective Covalent Attachment of Polymers. *Chem. Mater.* **2016**, *28*, 3318−3326.

(30) Chen, Y.; Espeel, P.; Reinicke, S.; Du Prez, F. E.; Stenzel, M. H. Control of Glycopolymer Nanoparticle Morphology by a One-Pot, Double Modification Procedure Using Thiolactones. *Macromol. Rapid Commun.* **2014**, *35*, 1128−1134.

(31) Marradi, M.; Chiodo, F.; García, I.; Penadés, S. Glyconanoparticles as Multifunctional and Multimodal Carbohydrate Systems. *Chem. Soc. Rev.* **2013**, *42*, 4728.

(32) Delbianco, M.; Bharate, P.; Varela-Aramburu, S.; Seeberger, P. H. Carbohydrates in Supramolecular Chemistry. *Chem. Rev.* **2016**, *116*, 1693−1752.

(33) Lundquist, J. J.; Toone, E. J. The Cluster Glycoside Effect. *Chem. Rev.* **2002**, *102*, 555−578.

(34) Pallarola, D.; Queralto, N.; Battaglini, F.; Azzaroni, O. Supramolecular Assembly of Glucose Oxidase on Concanavalin A—modified Gold Electrodes. *Phys. Chem. Chem. Phys.* **2010**, *12*, 8071.

(35) Ting, S. R. S.; Chen, G.; Stenzel, M. H. Synthesis of Glycopolymers and Their Multivalent Recognitions with Lectins. *Polym. Chem.* **2010**, *1*, 1392.

(36) Kottari, N.; Chabre, Y.; Sharma, R.; Roy, R. Multifaceted Development and Application of Biopolymers for Biology, Biomedicine and Nanotechnology. In *Advances in Polymer Science*; Dutta, P. K., Dutta, J., Eds.; Springer: Berlin, Heidelberg, 2013; Vol. *254*.

(37) Fasting, C.; Schalley, C. A.; Weber, M.; Seitz, O.; Hecht, S.; Koksch, B.; Dernedde, J.; Graf, C.; Knapp, E. W.; Haag, R. Multivalency as a Chemical Organization and Action Principle. *Angew. Chem., Int. Ed.* **2012**, *51*, 10472−10498.

(38) Ribeiro-Viana, R.; Sánchez-Navarro, M.; Luczkowiak, J.; Koeppe, J. R.; Delgado, R.; Rojo, J.; Davis, B. G. Virus-like Glycodendrinanoparticles Displaying Quasi-Equivalent Nested Polyvalency upon Glycoprotein Platforms Potently Block Viral Infection. *Nat. Commun.* **2012**, *3*, No. 1303.

(39) Richards, S. J.; Jones, M. W.; Hunaban, M.; Haddleton, D. M.; Gibson, M. I. Probing Bacterial-Toxin Inhibition with Synthetic Glycopolymers Prepared by Tandem Post-Polymerization Modification: Role of Linker Length and Carbohydrate Density. *Angew. Chem., Int. Ed.* **2012**, *51*, 7812−7816.

(40) Luczkowiak, J.; Muñoz, A.; Sánchez-Navarro, M. A.; Ribeiro-Viana, R.; Ginieis, A.; Illescas, B. M.; Martín, N.; Delgado, R.; Rojo, J. Glycofullerenes Inhibit Viral Infection. *Biomacromolecules* **2013**, *14*, 431−437.

(41) Li, H.; Lv, N.; Li, X.; Liu, B.; Feng, J.; Ren, X.; Guo, T.; Chen, D.; Fraser Stoddart, J.; Gref, R.; et al. Composite CD-MOF Nanocrystals-Containing Microspheres for Sustained Drug Delivery. *Nanoscale* **2017**, *9*, 7454−7463.

(42) Hartlieb, K. J.; Peters, A. W.; Wang, T. C.; Deria, P.; Farha, O. K.; Hupp, J. T.; Stoddart, J. F. Functionalised Cyclodextrin-Based Metal−organic Frameworks. *Chem. Commun.* **2017**, *53*, 7561−7564.

(43) Smaldone, R. A.; Forgan, R. S.; Furukawa, H.; Gassensmith, J. J.; Slawin, A. M. Z.; Yaghi, O. M.; Stoddart, J. F. Metalorganic Frameworks from Edible Natural Products. *Angew. Chem., Int. Ed.* **2010**, *49*, 8630−8634.

(44) Forgan, R. S. Metal-Organic Frameworks: Edible Frameworks. *Encyclopedia of Inorganic and Bioinorganic Chemistry*; John Wiley & Sons, Ltd.: Chichester, U.K., 2014; pp 1−13.

(45) Steber, J.; Guhl, W.; Stelter, N.; Schröder, F. R. Ecological Evaluation of Alkyl Polyglycosides. In *Alkyl Polyglycosides: Technology, Properties and Applications*; HiII, K., von Rybinski, W., Stoll, G., Eds.; Wiley-VCH Verlag GmbH & Co. KGaA: Weinheim, Germany, 1997; pp 177−190.

(46) Zhang, L.; Somasundaran, P.; Maltesh, C. Adsorption of N-Dodecyl-*β*-D-Maltoside on Solids. *J. Colloid Interface Sci.* **1997**, *191*, 202−208.

(47) Piccinini, E.; Pallarola, D.; Battaglini, F.; Azzaroni, O. Self-Limited Self-Assembly of Nanoparticles into Supraparticles: Towards Supramolecular Colloidal Materials by Design. *Mol. Syst. Des. Eng.* **2016**, *1*, 155−162.

(48) Xia, Y.; Nguyen, T. D.; Yang, M.; Lee, B.; Santos, A.; Podsiadlo, P.; Tang, Z.; Glotzer, S. C.; Kotov, N. A. Self-Assembly of Self-Limiting Monodisperse Supraparticles from Polydisperse Nanoparticles. *Nat. Nanotechnol.* **2011**, *6*, 580−587.

(49) Park, J. Il; Nguyen, T. D.; de Queirós Silveira, G.; Bahng, J. H.; Srivastava, S.; Zhao, G.; Sun, K.; Zhang, P.; Glotzer, S. C.; Kotov, N. A. Terminal Supraparticle Assemblies from Similarly Charged Protein Molecules and Nanoparticles. *Nat. Commun.* **2014**, *5*, No. 3593.

(50) Piccinini, E.; Pallarola, D.; Battaglini, F.; Azzaroni, O. Recognition-Driven Assembly of Self-Limiting Supramolecular Protein Nanoparticles Displaying Enzymatic Activity. *Chem. Commun.* **2015**, *51*, 14754−14757.

(51) Chuang, Y.-J.; Zhou, X.; Pan, Z.; Turchi, C. A Convenient Method for Synthesis of Glyconanoparticles for Colorimetric Measuring Carbohydrate−protein Interactions. *Biochem. Biophys. Res. Commun.* **2009**, *389*, 22−27.

(52) Banerjee, S. S.; Chen, D. Glucose-Grafted Gum Arabic Modified Magnetic Nanoparticles: Preparation and Specific Interaction with Concanavalin A. *Chem. Mater.* **2007**, *19*, 3667−3672.

(53) Borrebaeck, C.; Mattiasson, B. Lectin-Carbohydrate Interactions Studied by a Competitive Enzyme Inhibition Assay. *Anal. Biochem.* **1980**, *107*, 446−450.

(54) Moerz, S. T.; Kraegeloh, A.; Chanana, M.; Kraus, T. Formation Mechanism for Stable Hybrid Clusters of Proteins and Nanoparticles. *ACS Nano* **2015**, *9*, 6696−6705.

(55) Schreiber, A.; Huber, M. C.; Cölfen, H.; Schiller, S. M. Molecular Protein Adaptor with Genetically Encoded Interaction Sites Guiding the Hierarchical Assembly of Plasmonically Active Nanoparticle Architectures. *Nat. Commun.* **2015**, *6*, No. 6705.

(56) Hoshi, T.; Akase, S.; Anzai, J. I. Preparation of Multilayer Thin Films Containing Avidin through Sugar-Lectin Interactions and Their Binding Properties. *Langmuir* **2002**, *18*, 7024−7028.

(57) Sappia, L. D.; Piccinini, E.; Marmisollé, W.; Santilli, N.; Maza, E.; Moya, S.; Battaglini, F.; Madrid, R. E.; Azzaroni, O. Integration of Biorecognition Elements on PEDOT Platforms through Supramolecular Interactions. *Adv. Mater. Interfaces* **2017**, *4*, No. 1700502.

(58) Sauerbrey, G. Verwendung von Schwingquarzen Zur Wagung Dunner Schichten Und Zur Mikrowagung. *Z. Phys.* **1959**, *155*, 206−222.

(59) Kankaanpää, P.; Paavolainen, L.; Tiitta, S.; Karjalainen, M.; Päivärinne, J.; Nieminen, J.; Marjomäki, V.; Heino, J.; White, D. J. BioImageXD: An Open, General-Purpose and High-Throughput Image-Processing Platform. *Nat. Methods* **2012**, *9*, 683−689.

(60) Bruno, I. J.; Cole, J. C.; Edgington, P. R.; Kessler, M.; Macrae, C. F.; McCabe, P.; Pearson, J.; Taylor, R. New Software for Searching the Cambridge Structural Database and Visualizing Crystal Structures. *Acta Crystallogr., Sect. B: Struct. Sci., Cryst. Eng. Mater.* **2002**, *58*, 389−397.